CrossMark

Photon attenuation parameters for some tissues from Geant4 simulation, theoretical calculations and experimental data: a comparative study

Halil Arslan[1]

Abstract Mass attenuation coefficients, effective atomic numbers, effective electron densities and Kerma relative to air for adipose, muscle and bone tissues have been investigated in the photon energy region from 20 keV up to 50 MeV with Geant4 simulation package and theoretical calculations. Based on Geant4 results of the mass attenuation coefficients, the effective atomic numbers for the tissue models have been calculated. The calculation results have been compared with the values of the Auto-Z_{eff} program and with other studies available in the literature. Moreover, Kerma of studied tissues relative to air has been determined and found to be dependent on the absorption edges of the tissue constituent elements.

Keywords Attenuation coefficient · Effective atomic number · Geant4 simulation · Tissue model

1 Introduction

During more than three decades, due to the digital computing developments and wide use of radioactive sources, the attenuation measurements of X-rays and gamma rays have become an important part in numerous diverse fields of physics. Their interactions with the human tissues and organs have also occupied a special significance in medical physics by virtue of their applications in diagnostic and radiation therapy. Human organs are made of tissues that are formed by specialized cells. Each cell is composed of elements with low atomic numbers [1–3]. Therefore, the doses received by tissues imputed to ionization, scattering and absorption processes occured with such elements [4]. The mass attenuation coefficient (μ/ρ) and the mass energy-absorption coefficient (μ_{en}/ρ) need to be known for dosimetry studies. Such basic quantities are discussed in Sect. 3, and detailed information about them can be found in [5].

The first tabulations of the mass energy-absorption coefficient were the efforts of Berger [6] and Allison [7]. Berger's tabulation included 15 elements, air, and water at the energy region between 3 keV and 10 MeV, whereas Allison's tabulation for seven elements, air, and water for energies from 10 keV to 100 MeV. Later on, Hubbel published data [8] on mass attenuation and mass energy-absorption coefficients for H, C, N, O, Ar, and seven mixtures from 0.1 keV to 20 MeV. That work has been extended two times [9, 10] to cover all elements (for $Z = 1$ to 92) and 48 additional substances over a wide energy range from 1 keV to 20 MeV. As a technological alternative, the XCOM program was developed to calculate the attenuation coefficients of photon for elements, compounds, and mixtures over a wide range of energies [11]. This program has been converted to WinXcom software [12] based on the mixture rule for all elements and any mixture at selected energies. In addition, Chantler [13] provided new tabulation that was improved as a programme FFAST [14].

The Monte Carlo method is commonly used to simulate radiation interaction with matter and to obtain the mass attenuation coefficient. There are some strong toolkits like Geant4 and MCNP that are currently used in the field of radiation physics. The validation of Geant4 [15] simulation

✉ Halil Arslan
  harslan@sakarya.edu.tr

[1] Electrical and Electronics Engineering, Sakarya University of Applied Sciences, Sakarya, Turkey

package has been frequently examined for determining the attenuation coefficients by using different types of materials [16–19] and tissue-equivalent models [20, 21]. Moreover, this work is also a validation of Geant4 as a powerful alternative tool to calculate attenuation parameters. In addition to Geant4, MCNP is also preferred to simulate the attenuation of photon in various media and gives very satisfactory results (see, for example, [22–26]).

Effective atomic number (Z_{eff}), effective electron density (N_{eff}) and kinetic energy released per unit mass (Kerma) are also serviceable parameters to characterize photon interaction with human tissues. The variation of Z_{eff} with photon energies was suggested by Hine [27]. Thus, accurate and quick determinations of this parameter were targeted by several experiments, methods and programs. Such experiments, in which Z_{eff} is determined by using the attenuation coefficients, were performed for elements [28, 29], for mixtures [30–32] and for tissues or tissue-equivalent materials [33, 34]. In addition, many theoretical studies have been conducted to obtain the attenuation coefficients and effective atomic numbers for elements and mixtures. For example, Jayachandran found that the calculated value of the effective atomic number (7.23) for lithium tetraborate $Li_2B_4O_7$ agrees closely with the value of 7.22 for soft tissue of composition $C_5H_{40}O_{18}N$ [35]. Manohara, who investigated the effective atomic number for some fatty acids and cysteine, concluded that Z_{eff} is equal to the mean atomic number over a wide energy range around 1 MeV [36]. Singh, who studied dosimetric materials in terms of mass energy-absorption coefficients, equivalent atomic numbers and Kerma in the energy range between 0.015 and 15 MeV, concluded that Nylon has been found to be a good tissue substitute material for making tissue phantoms of the biological tissues [37]. Moreover, Taylor submitted the Auto-Z_{eff} software [38] as an appropriate method to evaluate the effective atomic numbers that necessitate consideration of energy-dependent behavior for composite materials such as biological tissues, alloys, polymers, compounds, and mixtures for total and partial photon interactions. Later on, Un and Caner developed a new platform (Direct-Z_{eff}) that computes the mass attenuation coefficients, the effective atomic numbers and the effective electron numbers per unit mass for any selected materials [39]. XMuDat is also a program to be used with Windows 95 or Windows NT operating systems for the evaluation of mass attenuation coefficient, mass energy-absorption coefficient and the single value of effective atomic number for a given material for total or specific reaction channels over range of 1 keV to 50 MeV [40]. Similar to the XMuDat, another program called NXcom is constructed for calculating attenuation coefficients of fast neutrons and gamma rays [41]. The results of the program were tested by comparing them with the ones from WinXcom and Monte Carlo simulations and show very good agreement. There are numerous studies in the literature (see, for instance, [42–49]) providing a wide database for attenuation coefficients, Z_{eff}, N_{eff} and Kerma for biomedical materials by using various methods and programs.

The present work shows the comparison between results from Geant4 simulation package, theoretical calculations and experiments for three different types of human tissues in terms of mass attenuation coefficients and effective atomic number. For this purpose, first of all, Geant4 Monte Carlo simulations have been utilized to extract the mass attenuation coefficients of photon for adipose, muscle and bone tissues. The results have been compared with the ones from theoretical calculations and experimental data available in the literature. Effective atomic numbers of studied tissue models have been computed by direct method, Auto-Z_{eff} and XMuDat programs. In addition, mean free paths of the photons, Kerma relative to air and effective electron density for those tissues have been discussed.

2 Geant4 simulation

Monte Carlo simulations of this study have been performed by using the package of Geant4.10.03.p02. Geant4 is the successor of the GEANT series of software toolkits that were first to use object-oriented programming based on C++ language. It allows users to define classes for the detector geometry, primary particle generator, and physics processes to handle the interactions of particles with matter. It provides a set of electromagnetic physics processes handling the photon-tissue interactions (photoelectric effect, Compton scattering, Rayleigh scattering and pair production) over a wide range of energy [50].

In this study, adipose, muscle and bone tissue models have been studied by the Geant4 code that was explained in detail in our previous work [51]. Briefly, they have been considered to have simple geometries, slabs of various thicknesses from 1 to 10 cm. The elemental composition of the studied tissues is shown in Table 1. The densities of tissue models have been chosen to be $0.95 \, g/cm^3$ for adipose tissue, $1.04 \, g/cm^3$ for muscle tissue and $1.85 \, g/cm^3$ for bone tissue [1, 3].

The beam source has been positioned on one of the edges of the tissue model such that the momentum directions of the photons are perpendicular to the tissue surface. Simulations have been performed for 14 different photon energies from 20 keV to 50 MeV, for each tissue type separately. For each run, 10^6 incident photons have been injected upon the tissue models.

Table 1 Fraction weights of the elements for adipose, muscle and bone tissues

Element		Tissue		
Z	Symbol	Adipose	Muscle	Bone
1	H	0.1140	0.1020	0.0640
6	C	0.5980	0.1230	0.2780
7	N	0.0070	0.0350	0.0270
8	O	0.2780	0.7290	0.4100
11	Na	0.0010	0.0008	–
12	Mg	–	0.0002	0.0020
15	P	–	0.0020	0.0700
16	S	0.0010	0.0050	0.0020
17	Cl	0.0010	–	–
19	K	–	0.0030	–
20	Ca	–	–	0.1470

3 Methods of calculation

3.1 Mass attenuation coefficient

A beam of photons with an incident intensity, I_0, penetrating a layer of material with thickness, x, and density, ρ, emerges with intensity, I, given by the exponential attenuation law:

$$I/I_0 = e^{-\mu x}, \tag{1}$$

where μ in the unit of cm^{-1} is the linear attenuation coefficient of the absorber, which can be obtained from measured values of I_0, I and x. In addition, the ratio of the linear attenuation coefficient to the density (μ/ρ) is called the mass attenuation coefficient. μ/ρ relies heavily on theoretical values for the total cross section per atom (σ_{tot}) according to the equation:

$$\mu/\rho = \sigma_{tot}/uA, \tag{2}$$

where u is the atomic mass unit and A is the atomic mass number of the target element. The total cross section can be written as the sum over contributions from the principal photon interactions by

$$\sigma_{tot} = \sigma_{ph} + \sigma_{coh} + \sigma_{incoh} + \sigma_{pair}, \tag{3}$$

where σ_{ph} is the atomic photo-effect cross section, σ_{coh} and σ_{incoh} are the coherent (Rayleigh) and the incoherent (Compton) scattering cross sections, respectively, and σ_{pair} is the cross sections for electron-positron production. The total mass attenuation coefficient, $(\mu/\rho)_{tot}$, for any chemical compound or mixture of elements is given by mixture rule.

$$(\mu/\rho)_{tot} = \sum_i w_i (\mu/\rho)_i, \tag{4}$$

w_i and $(\mu/\rho)_i$ are the weight fraction and mass attenuation coefficient of the ith constituent element, respectively.

3.2 Effective atomic number

Z_{eff} has been calculated as a function of photon energy by using three different methods: direct method, interpolation method and Auto-Z_{eff} program. In addition, XMuDat software has also been utilized to get Z_{eff} value.

According to the direct method, Z_{eff} is equal to ratio of total atomic cross section (σ_a) and total electronic cross section (σ_e).

$$Z_{eff} = \sigma_a/\sigma_e \tag{5}$$

The total atomic cross section, σ_a, is given by:

$$\sigma_a = \frac{(\mu/\rho)_{tissue}}{N_A \sum_i (\frac{w_i}{A_i})}, \tag{6}$$

where N_A is the Avogadro's number. For calculations, the mass attenuation coefficients have been accepted to have values estimated based on Geant4 simulation. The electronic cross section, σ_e, is defined as:

$$\sigma_e = \frac{1}{N_A} \sum_i \left[\frac{f_i A_i}{Z_i} (\mu/\rho)_i \right], \tag{7}$$

where f_i and Z_i are the fractional abundance (mass fraction) and the atomic number of the ith element in the tissue, respectively. The effective electron density (N_{eff}) is the number of electrons per unit mass and expressed by the relation of:

$$N_{eff} = \frac{(\mu/\rho)_{tissue}}{\sigma_e}. \tag{8}$$

The Auto-Z_{eff} program is an user friendly interface used to compute energy-dependent atomic numbers with very low uncertainties for user-specified material. The cross section matrices of photon-element interactions are constructed for energies between 0.01 and 1000 MeV. Coefficients for composite media are constructed via linear additivity of the fractional constituents and contrasted against the precalculated matrices at each energy, thereby associating an effective atomic number through interpolation of adjacent cross section data.

XMuDat computer software is able to produce a single-valued effective atomic number for a given material by assuming the photoelectric effect as the main interaction process [40]. The method of XMuDat program to calculate the effective atomic number based on the formula:

$$Z_{\text{eff}} = \sum_i (\alpha_i Z_i^{m-1})^{1/(m-1)}, \tag{9}$$

where α_i is the fractional number of the electrons of the ith element and m is a constant between 3 and 5. It is preferred that m is set to be 3.6 for elements with $Z < 6$ and 4.1 for elements with $Z > 6$ [52].

3.3 Kerma

Kerma is the initial kinetic energy of all secondary charged particles liberated per unit mass. It is applicable to photons and neutrons and in the unit of $J\,kg^{-1} = Gy$, as the absorbed dose. Kerma of the compounds, mixtures, and human tissues relative to air was calculated [47, 53, 54] based on the relation:

$$K_r = \frac{K_{\text{tissue}}}{K_{\text{air}}} = \frac{(\mu_{\text{en}}/\rho)_{\text{tissue}}}{(\mu_{\text{en}}/\rho)_{\text{air}}}, \tag{10}$$

where (μ_{en}/ρ) is the mass energy-absorption coefficient. In this work, the values of (μ_{en}/ρ) for the elements of studied tissues have been extracted from the compilation of Hubbell [9], and then the values of (μ_{en}/ρ) for the tissues have been calculated by mixture rule.

4 Result and discussion

4.1 Mass attenuation coefficient

The exponential relationship between the ratio of transmitted photon intensity to that of the incident photons (I/I_0), which is called transmittance, and the tissue thickness is given by Eq. 1. Geant4 simulation results I/I_0 with energies from 0.02 MeV to 50 MeV have been plotted as functions of tissue thicknesses for adipose, muscle and bone tissue models separately (see Fig. 1). Each graph has been fitted to the function of $e^{-\mu x}$ in order to get the fitting parameter, μ (linear attenuation coefficient). The solid lines in the graphs are the fit curves.

The mass attenuation coefficient (μ/ρ) for each tissue type and energy has been calculated by dividing μ to the density of the tissue of interest. μ/ρ values for adipose, muscle and bone tissues obtained from the simulation are given in Tables 2, 3 and 4, respectively, together with the ones from theoretical calculations and experimental studies.

It can be seen from the tables that the results obtained from simulation, theoretical and experimental studies are in a very good agreement. Generally, the errors on the values from the simulations and the experiments were calculated to be less than 2% and 3%, respectively [21, 33]. In the present study, error propagation of the fitting in the

figures has been found to be less than 5%. The small discrepancies among the values can be attributed to the tissue modeling and the methods that were used to estimate the cross sections. The μ/ρ values decrease with increasing photon energies for all tissue types. This behavior depends on the total photon interaction that shows the superposition of multiple partial interactions (e.g. photoelectric absorption, Compton scattering and pair production). According to theoretical calculations, the mass attenuation coefficients experience a significant attenuation of 71.64 % for adipose tissue, 77.73 % for muscle tissue and 84.47 % for bone tissue in the energy region between 20 and 30 keV. The calculated theoretical μ/ρ values tend to be higher than the simulated values for low energies. However, these values show more agreement at a high energy region. It is clear that the higher theoretical values reflect the effect of the chemical composition of the tissue models and the mixture rule method.

The photoelectric absorption is a dominant process for photon energies of less than 50 keV. In this energy region, the value of the mass attenuation coefficients rapidly goes down due to the photoelectric cross sections directly proportional to Z^4 and inversely to E^3. At higher energies, the Compton scattering becomes the dominant mechanism that varies with Z and E^{-1}. Therefore, a smooth decrease of μ/ρ values was observed. For the photon energies greater than 1022 keV, the pair-production process appears and the interaction cross section changes with Z^2 and $\log E$. Thus, the μ/ρ values look independent of photon energy and decrease slowly.

Mean free path (λ), defined as the average distance between two successive interactions, is simply reciprocal of the linear attenuation coefficient. λ of the photons through adipose, muscle and bone tissues is illustrated in Fig. 2 as a function of energy.

It is clear that λ values increase with energy except for the abrupt changes near the absorption edges and at the threshold energy of photon interactions, such as photoelectric effect, coherent (Rayleigh), incoherent scattering, and electron-positron production. The λ is inversely proportional with the number of photon collisions. Thus, it can be concluded that the photon collisions are relatively high in the low energy region < 30 keV, which makes the mass attenuation coefficients bigger. This property is also an explanation for the fact that the low energy X-rays deposit much energy (radiation dose) in the first few centimeters in the body. For higher energies, the number of collisions sharply drops down causing a decrease in the mass attenuation coefficients.

Fig. 1 Transmittances as a function of tissue thickness for adipose, muscle and bone tissues with fit curves
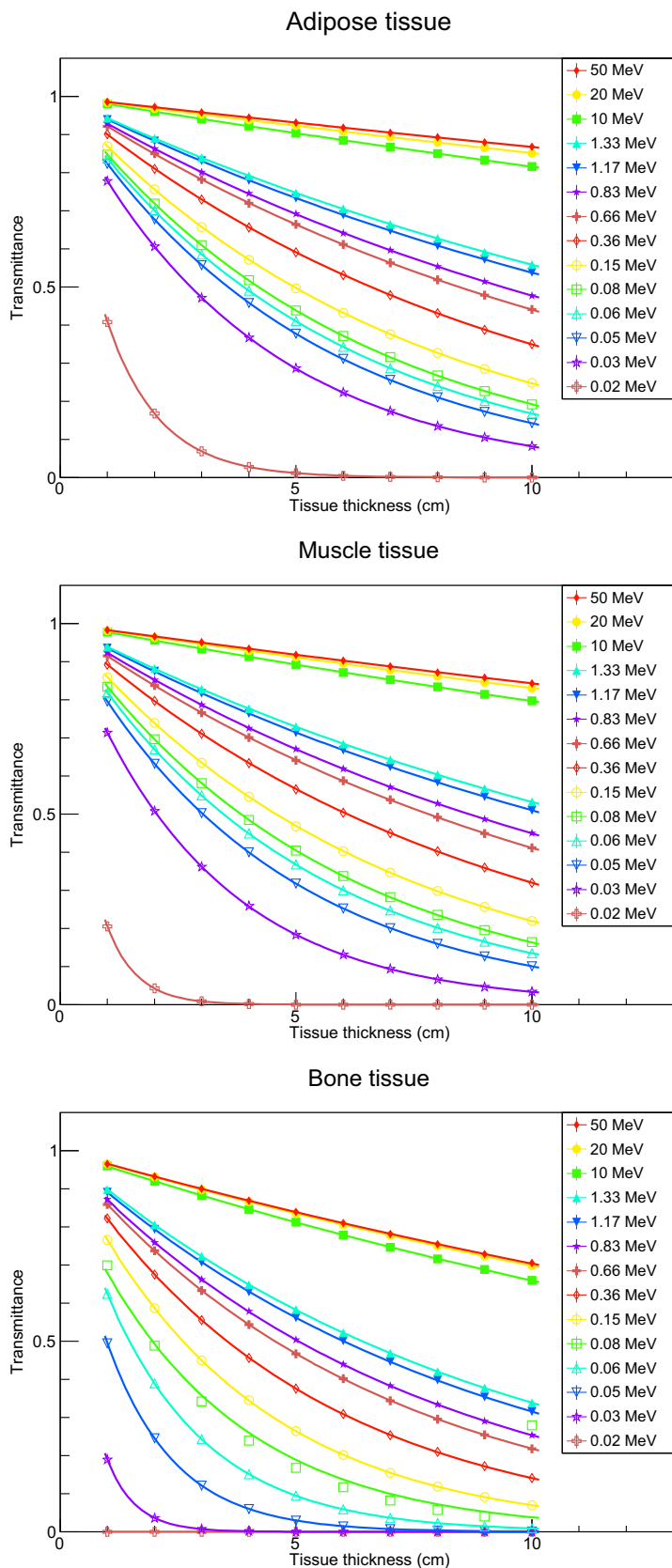
Table 2 Mass attenuation coefficients for adipose tissue

Photon energy (MeV)	Mass attenuation coefficients (cm²/g)		
	Theoretical	Simulation	Experiment
0.02	1.079	0.939	1.26 [33]
0.03	0.306	0.264	0.32 [33]
0.05	0.223	0.205	0.21 [33]
0.06	0.198	0.187	–
0.08	0.179	0.173	0.18 [34]
0.15	0.150	0.148	–
0.36	0.111	0.111	–
0.66	0.086	0.088	0.08 [34]
0.83	0.077	0.076	0.07 [34]
1.17	0.065	0.066	0.06 [34]
1.33	0.061	0.062	0.05 [34]
10	0.021	0.020	–
20	0.017	0.014	–
50	0.015	0.017	–

Table 4 Mass attenuation coefficients for bone tissue

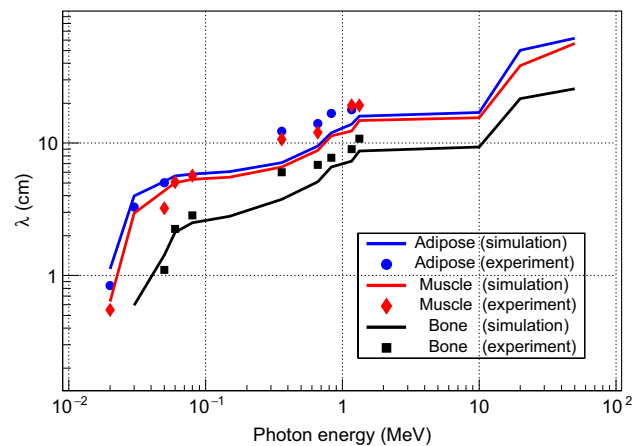| Photon energy (MeV)	Mass attenuation coefficients (cm²/g)		
	Theoretical	Simulation	Experiment
0.02	6.325	–	–
0.03	0.982	0.910	–
0.05	0.419	0.379	0.49 [33]
0.06	0.278	0.255	0.24 [33]
0.08	0.207	0.193	0.19 [21]
0.15	0.149	0.144	–
0.36	0.107	0.106	0.09 [21]
0.66	0.082	0.082	0.08 [21]
0.83	0.074	0.074	0.07 [21]
1.17	0.062	0.062	0.06 [21]
1.33	0.058	0.058	0.05 [21]
10	0.023	0.025	–
20	0.20	0.021	–
50	0.019	0.019	–

Table 3 Mass attenuation coefficients for muscle tissue

Photon energy (MeV)	Mass attenuation coefficients (cm²/g)		
	Theoretical	Simulation	Experiment
0.02	1.702	1.517	1.75 [33]
0.03	0.379	0.325	–
0.05	0.244	0.221	0.30 [33]
0.06	0.206	0.192	0.19 [33]
0.08	0.182	0.174	0.17 [21]
0.15	0.149	0.146	–
0.36	0.110	0.109	0.09 [21]
0.66	0.085	0.085	0.08 [21]
0.83	0.076	0.078	–
1.17	0.065	0.065	0.05 [21]
1.33	0.061	0.062	0.05 [21]
10	0.022	0.025	–
20	0.018	0.017	–
50	0.017	0.012	–

Fig. 2 Mean free path (λ) of photon through adipose, muscle and bone tissues

4.2 Effective atomic numbers

The effective atomic numbers (Z_{eff}) for adipose, muscle and bone tissues in the photon energy region 0.01 to 20 MeV are shown in Fig. 3.

It was found that the computed effective atomic numbers at a low energy region (< 30 keV) have a high uncertainty. For example, it reaches the value of $\pm 25\%$ when Auto-Z_{eff} is utilized [38]. On the other hand, the

effective atomic numbers calculated by using the Auto-Z_{eff} software and direct method are in a very good agreement in the energy region from 50 keV to 10 MeV where the Compton scattering is a dominant process. In this medium-energy region, the effective atomic numbers have been observed to be constant, whereas significant variations have been found in the lower (< 50 keV) as well as in the higher (> 10 MeV) regions. The effective atomic numbers calculated by using the direct method have higher values than those computed by Auto-Z_{eff} software and interpolation method in the energy regions of both photo-absorption and pair production. Moreover, the Z_{eff} calculated by direct method and Auto-Z_{eff} program have a maximum differences of 18.9% for adipose, 21.2% for muscle and 38.7%

Fig. 3 Effective atomic number as a function of photon energy for adipose, muscle and bone tissues
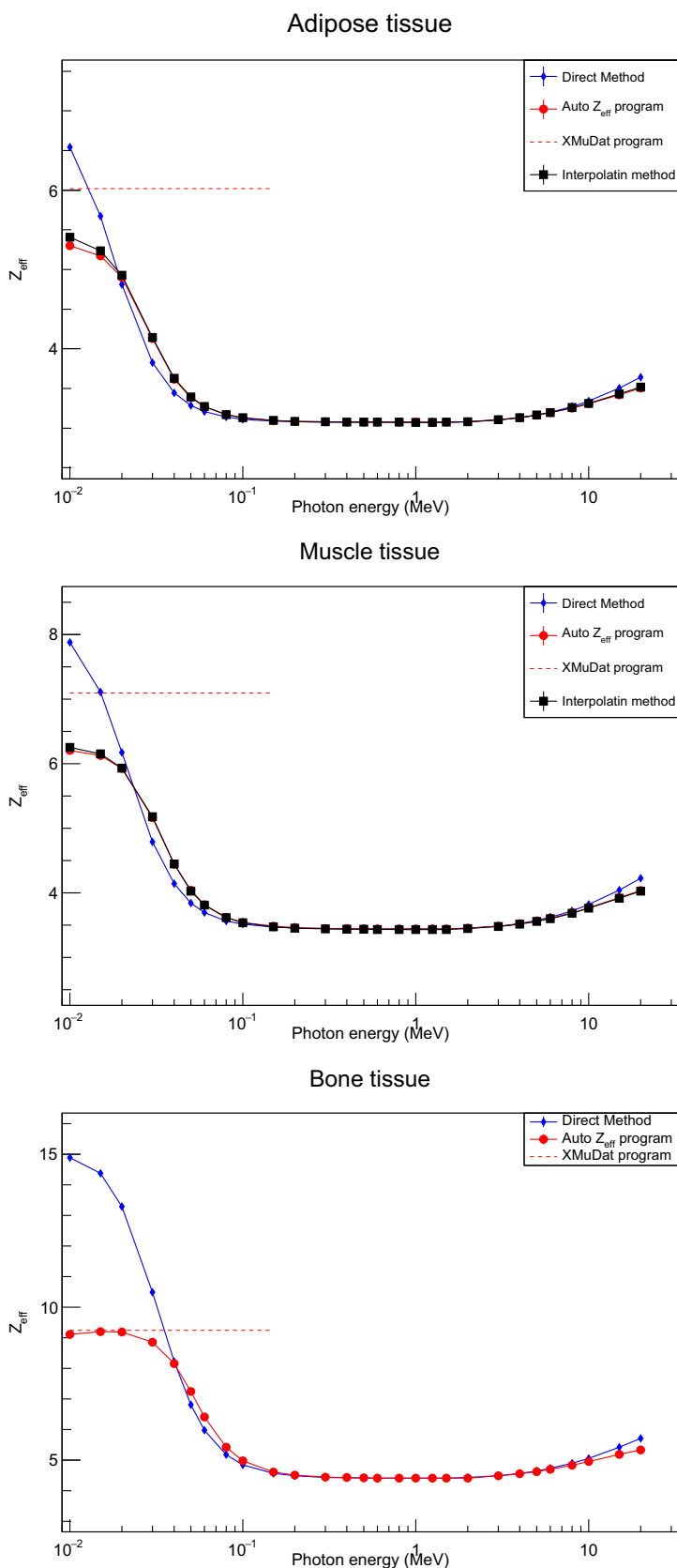
for bone in the energy region around 10 keV. The values of Z_{eff} for adipose and muscle by using interpolation method were taken from [44]. Furthermore, the single Z_{eff} values obtained from the XMuDat program are also included to the graphs shown in Fig. 3. For each type of tissue, it lies between the values obtained from the direct method and the one from Auto-Z_{eff} software.

The plot of effective atomic numbers versus effective electron densities for tissue models is shown in Fig. 4. As it can be expected, the relation between N_{eff} and Z_{eff} is smooth and linear since they are directly proportional with each other.

4.3 Kerma

Kerma relative to air (K_{r}) as a function of photon energy for adipose, muscle and bone tissues over the energy range from 1 keV to 20 MeV is shown in Fig. 5.
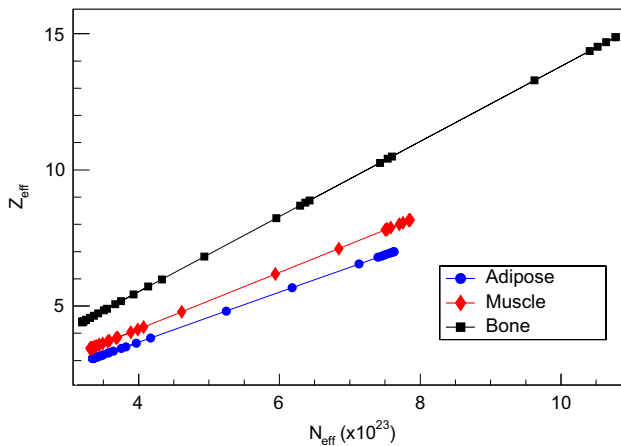
Fig. 4 Effective atomic numbers versus Effective electron densities for adipose, muscle and bone tissues
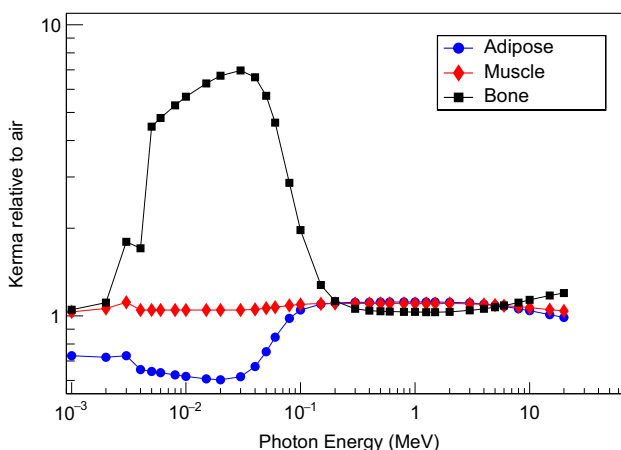
Fig. 5 Kerma relative to air as a function of photon energy for adipose, muscle and bone tissues

Energy-dependent variation of K_{r} represents the behavior of Z_{eff} due to different processes such as photo-absorption, Compton effect and pair production. Although this variation can be seen clearly at a photon energy below 100 keV, the K_{r} values were found to be constant ($\sim$ unity) for higher energies. The K_{r} value for bone tissue, which contains the higher-Z elements like Ca, reaches up to 6.96 at 40 keV. This peak value of K_{r} can be attributed to the photoelectric effect around the K-absorption edge of Ca. For muscle and adipose tissues, which have negligible fraction weights of high-Z elements, the values of K_{r} are equal or less than one.

5 Conclusion

This article provides data, from Geant4 simulations and theoretical calculations, of mass attenuation coefficients and effective atomic numbers for adipose, muscle and bone tissues over a wide range of energies up to 50 MeV. All of these parameters are mainly dependent on the incident photon energy and the tissue constituent elements. The mass attenuation coefficient and effective atomic numbers sharply decrease where the photo-absorption is the dominant mechanism in tissue. Also, they are nearly constant at the predominance of the Compton scattering, and a smooth variation can be seen at the energy region of the pair-production process.

Mass attenuation coefficients generated by using Geant4 have uncertainties less than $\pm 1\%$ at the low energy region and less than 8% at high energies. Effective atomic numbers calculated by direct method and Auto-Z_{eff} program have a maximum difference of 18.9% for adipose, 21.2% for muscle and 38.7% for bone in the energy region around 10 keV. The single effective atomic number obtained by the XMuDat program exhibited values higher than those of the Auto-Z_{eff} program and less than those of the direct method. Moreover, the elements that compose the tissue play a significant role in the calculation of Kerma.

References

1. ICRP, *Basic Anatomical and Physiological Data for Use in Radiological Protection: Reference Values*. ICRP Publication 89. Ann. ICRP 32 (2003)
2. Y.S. Kim, Human tissues: chemical composition and photon dosimetry data. Radiat. Res. **57**(1), 38–45 (1974). https://doi.org/10.2307/3573753
3. D.R. White J. Booz, R.V. Griffith et al., ICRU Report 44: tissue substitutes in radiation dosimetry and measurement. J. ICRU os23 (1989). https://doi.org/10.1093/jicru/os23.1.Report44

4. Y. Elmahroug, B. Tellili, C. Souga et al., Determination of total mass attenuation coefficients, effective atomic numbers and electron densities for different shielding materials. Ann. Nucl. Energy **75**, 268–274 (2015). https://doi.org/10.1016/j.anucene.2014.08.015

5. A. McNair, ICRU Report 33: radiation quantities and units. J. Label Compd. Radiopharm. **18**, 1398 (1981). https://doi.org/10.1002/jlcr.2580180918

6. R.T. Berger, The X- or gamma-ray energy absorption or transfer coefficient: tabulations and discussion. Radiat. Res. **15**, 1–29 (1961). https://doi.org/10.2307/3571063

7. J.W. Allison, Gamma-radiation absorption coefficients of various materials allowing for Bremsstrahlung and other secondary radiations. Aust. J. Phys. **14**, 443–461 (1961). https://doi.org/10.1071/PH610443

8. J.H. Hubbell, Photon mass attenuation and mass energy-absorption coefficients for H, C, N, O, Ar, and seven mixtures from 0.1 keV to 20 MeV. Radiat. Res. **70**, 58–81 (1977). https://doi.org/10.2307/3574732

9. J.H. Hubbell, Photon mass attenuation and energy-absorption coefficients. Int. J. Appl. Radiat. Isot. **33**(11), 1269–1290 (1982). https://doi.org/10.1016/0020-708X(82)90248-4

10. J.H. Hubbell, S.M. Seltzer, Tables of X-ray mass attenuation coefficients and mass energy-absorption coefficients 1 keV to 20 MeV for elements Z =1 to 92 and 48 additional substances of Dosimetric Interest. NIST Standard Reference Database 126 (1995). https://doi.org/10.18434/T4D01F

11. M.J. Berger, J.H. Hubbell, S.M. Seltzer et al., XCOM: photon cross sections database. NIST Standard Reference Database 8 (1998). https://doi.org/10.18434/T48G6X

12. L. Gerward, N. Guilbert, K.B. Jensen et al., WinXCom—a program for calculating X-ray attenuation coefficients. Radiat. Phys. Chem. **71**(2004), 653–654 (2004). https://doi.org/10.1016/j.radphyschem.2004.04.040

13. C.T. Chantler, Theoretical form factor, attenuation, and scattering tabulation for Z = 1–92 from E = 1–10 eV to E = 0.4–1.0 MeV. J. Phys. Chem. Ref. Data **24**(1), 71–643 (1995). https://doi.org/10.1063/1.555974

14. C.T. Chantler et al., X-ray form factor, attenuation and scattering tables. NIST Standard Reference Database 66 (2005). https://doi.org/10.18434/T4HS32

15. S. Agostinelli, J. Allison, K. Amako et al., GEANT4—a simulation toolkit. Nucl. Instrum. Methods Phys. Res. A **506**(3), 250–303 (2003). https://doi.org/10.1016/S0168-9002(03)01368-8

16. M.E. Medhat, Y. Wang, Geant4 code for simulation attenuation of gamma rays through scintillation detectors. Ann. Nucl. Energy **62**, 316–320 (2013). https://doi.org/10.1016/j.anucene.2013.06.034

17. V.P. Singh, M.E. Medhat, N.M. Badiger, Photon attenuation coefficients of thermoluminescent dosimetric materials by Geant4 toolkit, XCOM program and experimental data: a comparison study. Ann. Nucl. Energy **68**, 96–100 (2014). https://doi.org/10.1016/j.anucene.2014.01.011

18. S.S. Obaid, M.I. Sayyed, D.K. Gaikwad et al., Photon attenuation coefficients of different rock samples using MCNPX, Geant4 simulation codes and experimental results: a comparison study. Radiat. Eff. Defect Solids **173**(11–12), 900–914 (2018). https://doi.org/10.1080/10420150.2018.1505890

19. A. Kumar, S.P. Singh, Y. Elmahroug et al., Gamma ray shielding studies on 26.66 B_2O_3–16GeO$_2$–4Bi$_2$O$_3$–(53.3−x)PbO–xPbF$_2$ glass system using MCNPX, Geant4 and XCOM. Mater. Res. Express **5**(9), 095203 (2018). https://doi.org/10.1088/2053-1591/aad821

20. R.M. Lokhande, B.S. Surung, P.P. Pawar, Measurement of effective atomic number and electron density of carbohydrates by using NIST, Geant4 and NaI(Tl): a comparative study. Int. J. Adv. Res. **5**(5), 1733–1740 (2017). https://doi.org/10.21474/IJAR01/4303

21. M.E. Medhat, S.P. Shirmardi, V.P. Singh, Comparison of Geant 4, MCNP simulation codes of studying attenuation of gamma rays through biological materials with XCOM and experimental data. J. Appl. Comput. Math. **3**(6), 1000179 (2014). https://doi.org/10.4172/2168-9679.1000179

22. M.I. Sayyed, H.O. Tekin, E.E. Altunsoy et al., Radiation shielding study of tellurite tungsten glasses with different antimony oxide as transparent shielding materials using MCNPX code. J. Non-Cryst. Solids **498**, 167–172 (2018). https://doi.org/10.1016/j.jnoncrysol.2018.06.022

23. B.O. Elbashir, M.G. Dong, M.I. Sayyed et al., Comparison of Monte Carlo simulation of gamma ray attenuation coefficients of amino acids with XCOM program and experimental data. Results Phys. **9**, 6–11 (2018). https://doi.org/10.1016/j.rinp.2018.01.075

24. M.I. Sayyed, S.A.M. Issa, M. Büyükyildiz et al., Determination of nuclear radiation shielding properties of some tellurite glasses using MCNP5 code. Radiat. Phys. Chem. **150**, 1–8 (2018). https://doi.org/10.1016/j.radphyschem.2018.04.014

25. K. Verdipoor, A. Alemi, A. Mesbahi, Photon mass attenuation coefficients of a silicon resin loaded with WO$_3$, PbO, and Bi$_2$O$_3$ micro and nano-particles for radiation shielding. Radiat. Phys. Chem. **147**, 85–90 (2018). https://doi.org/10.1016/j.radphyschem.2018.02.017

26. A. Mesbahi, H. Ghiasi, Shielding properties of the ordinary concrete loaded with micro- and nano-particles against neutron and gamma radiations. Appl. Radiat. Isot. **136**, 27–31 (2018). https://doi.org/10.1016/j.apradiso.2018.02.004

27. G.J. Hine, The effective atomic numbers of materials for various gamma ray interactions. Phys. Rev **85**, 725–737 (1952)

28. M.T. Islam, N.A. Rae, J.L. Glover et al., Measurement of the X-ray mass attenuation coefficients of gold in the 38–50-keV energy range. Phys. Rev. A **81**, 022903 (2010). https://doi.org/10.1103/PhysRevA.81.022903

29. B. Goswami, N. Chaudhuri, Measurements of gamma-ray attenuation coefficients. Phys. Rev. A **7**, 1912–1916 (1973). https://doi.org/10.1016/0029-554X(73)90358-3

30. B.S. Sidhu, A.S. Dhaliwal, K.S. Mann et al., Study of mass attenuation coefficients, effective atomic numbers and electron densities for some low Z compounds of dosimetry interest at 59.54 keV incident photon energy. Ann. Nucl. Energy **42**, 153–157 (2012). https://doi.org/10.1016/j.anucene.2011.12.015

31. H. Buhr, L. Büermann, M. Gerlach et al., Measurement of the mass energy-absorption coefficient of air for X-rays in the range from 3 to 60 keV. Phys. Med. Biol. **57**(24), 8231–8247 (2012). https://doi.org/10.1088/0031-9155/57/24/8231

32. B. Akça, S.Z. Erzeneoğlu, The mass attenuation coefficients, electronic, atomic, and molecular cross sections, effective atomic numbers, and electron densities for compounds of some biomedically important elements at 59.5 keV. Sci. Technol. Nucl. Install. 901465 (2014). https://doi.org/10.1155/2014/901465

33. W. Geraldelli, A. Tomal, M.E. Poletti, Characterization of tissue-equivalent materials through measurements of the linear attenuation coefficient and scattering profiles obtained with polyenergetic beams. IEEE Trans. Nucl. Sci. **60**(2), 566–571 (2013). https://doi.org/10.1109/TNS.2013.2248382

34. N.A.B. Amin, J. Zukhi, N.A. Kabir et al., Determination of effective atomic number s from mass attenuation coefficients of tissue-equivalent materials in the energy range 60 keV–1.33 MeV. J. Phys. Conf. Ser. **851**, 012018 (2017). https://doi.org/10.1088/1742-6596/851/1/012018

35. C.A. Jayachandran, Calculated effective atomic number and Kerma values for tissue-equivalent and dosimetry materials. Phys. Med. Biol. **16**(4), 617–623 (1971). https://doi.org/10.1088/0031-9155/16/4/005

36. S.R. Manohara, S.M. Hanagodimath, K.S. Thind et al., The effective atomic number revisited in the light of modern photon-interaction cross-section databases. Appl. Radiat. Isot. **68**(4–5), 784–787 (2010). https://doi.org/10.1016/j.apradiso.2009.09.047

37. K.S. Mann, M. Kurudirek, G.S. Sidhu, Verification of dosimetric materials to be used as tissue-substitutes in radiological diagnosis. Appl. Radiat. Isot. **70**(4), 681–691 (2012). https://doi.org/10.1016/j.apradiso.2011.12.008

38. M.L. Taylor, R.L. Smith, F. Dossing et al., Robust calculation of effective atomic numbers: the Auto-Zeff software. Med. Phys. **39**(4), 1769–1778 (2012). https://doi.org/10.1118/1.3689810

39. A. Un, T. Caner, The direct-Z_{eff} software for direct calculation of mass attenuation coefficient, effective atomic number and effective electron number. Ann. Nucl. Energy **65**, 158–165 (2014). https://doi.org/10.1016/j.anucene.2013.10.041

40. R. Nowotny, XMuDat: photon attenuation data on PC. IAEA Report IAEA-NDS 195 (1998)

41. A.M. El-Khayatt, NXcom—a program for calculating attenuation coefficients of fast neutrons and gamma-rays. Ann. Nucl. Energy **38**(1), 128–132 (2011). https://doi.org/10.1016/j.anucene.2010.08.003

42. H.C. Manjunatha, B. Rudraswamy, Study of effective atomic number and electron density for tissues from human organs in the energy range of 1 keV–100 GeV. Health Phys. **104**(2), 158–162 (2013). https://doi.org/10.1097/HP.0b013e31827132e3

43. M. Kurudirek, Effective atomic numbers, water and tissue equivalence properties of human tissues, tissue equivalents and dosimetric materials for total electron interaction in the energy region 10 keV–1 GeV. Appl. Radiat. Isot. **94**, 1–7 (2014). https://doi.org/10.1016/j.apradiso.2014.07.002

44. V.R. Shivaramu, Effective atomic number for photon energy absorption and photon attenuation of tissues from human organs. Med. Dosim. **27**, 1–9 (2002). https://doi.org/10.1016/S0958-3947(01)00078-4

45. V.P. Singh, N.M. Badiger, N. Kucuk, Assessment of methods for estimation of effective atomic numbers of common human organ and tissue substitutes: waxes, plastics and polymers. Radioprotection **49**(2), 115–121 (2014). https://doi.org/10.1051/radiopro/2013090

46. M. Kurudirek, T. Onaran, Calculation of effective atomic number and electron density of essential biomolecules for electron, proton, alpha particle and multi-energetic photon interactions. Radiat. Phys. Chem. **112**, 125–138 (2015). https://doi.org/10.1016/j.radphyschem.2015.03.034

47. D. Salehi, D. Sardari, M.S. Jozani, Investigation of some radiation shielding parameters in soft tissue. J. Radiat. Res. Appl. Sci. **8**(3), 439–445 (2015). https://doi.org/10.1016/j.jrras.2015.03.004

48. M. Kurudirek, Effective atomic number of soft tissue, water and air for interaction of various hadrons, leptons and isotopes of hydrogen. Int. J. Radiat. Biol. **93**(12), 1299–1305 (2017). https://doi.org/10.1080/09553002.2018.1388546

49. D.K. Gaikwad, M.I. Sayyed, S.S. Obaid et al., Gamma ray shielding properties of TeO_2–ZnF_2–As_2O_3–Sm_2O_3 glasses. J. Alloys Compd. **765**, 451–458 (2018). https://doi.org/10.1016/j.jallcom.2018.06.240

50. J. Apostolakis, A. Bagulya, S. Elles et al., Validation and verification of Geant4 standard electromagnetic physics. J. Phys. Conf. Ser. **219**, 032044 (2010). https://doi.org/10.1088/1742-6596/219/3/032044

51. B.T. Tonguc, H. Arslan, M.S. Al-Buriahi, Studies on mass attenuation coefficients, effective atomic numbers and electron densities for some biomolecules. Radiat. Phys. Chem. **153**, 86–91 (2018). https://doi.org/10.1016/j.radphyschem.2018.08.025

52. D.F. Jackson, H.J. David, X-ray attenuation coefficients of elements and mixtures. Phys. Rep. **70**, 169–233 (1981). https://doi.org/10.1016/0370-1573(81)90014-4

53. S.R. Manohara, S.M. Hanagodimath, L. Gerward, Studies on effective atomic number, electron density and kerma for some fatty acids and carbohydrates. Phys. Med. Biol. **53**(20), N377–86 (2008). https://doi.org/10.1088/0031-9155/53/20/N01

54. D. Yilmaz, Y. Şahin, L. Demir, Studies on mass attenuation coefficient, mass energy absorption coefficient, and kerma for Fe alloys at photon energies of 17.44 to 51.70 keV. Turk. J. Phys. **39**(1), 81–90 (2015). https://doi.org/10.3906/fiz-1408-4